

Figure 3. Partial pressures in an ampule containing 1 mol of  $\text{InCl}_3/22.4$  L: —, excess  $\text{NiCl}_2$ ; ---, 0.02 mol of  $\text{NiCl}_2/22.4$  L.

For comparison, thermodynamic data related to the formation of gaseous complexes in the  $\text{NiCl}_2/\text{InCl}_3$  and in the  $\text{CoCl}_2/\text{InCl}_3$  systems are collected in Table IV. Within the limits of error, the enthalpies of adding the first and second  $\text{InCl}_3(\text{g})$  to  $\text{NiCl}_2(\text{g})$  are the same,  $-36 \pm 2$  kcal mol $^{-1}$ , but they are significantly less negative than for the addition of

$\text{InCl}_3(\text{g})$  to  $\text{CoCl}_2(\text{g})$ . The same sequence of stability is observed in the dimerization of  $\text{CoCl}_2(\text{g})$ <sup>14</sup> and  $\text{NiCl}_2(\text{g})$ <sup>15</sup> (Table IV), but there the coordination is the same for both metals while here it appears to be different for  $\text{CoIn}_2\text{Cl}_6(\text{g})$  and  $\text{NiIn}_2\text{Cl}_6(\text{g})$ . We have no proposition for reconciling the low stability of  $\text{NiL}_2\text{Cl}_6(\text{g})$  with its apparently octahedral  $\text{NiCl}_6$  center.

**Acknowledgment.** This project has been supported by the Swiss National Science Foundation (Grant 2.359-0.75).

**Registry No.**  $\text{NiIn}_2\text{Cl}_6$ , 63950-50-5;  $\text{NiInCl}_5$ , 63950-49-2;  $\text{NiCl}_2$ , 7718-54-9;  $\text{InCl}_3$ , 10025-82-8;  $\text{In}_2\text{Cl}_6$ , 21563-01-9.

#### References and Notes

- (1) H. Schäfer, *Angew. Chem.*, **88**, 775 (1976).
- (2) F. Dienstbach and F. P. Emmenegger, *Helv. Chim. Acta*, **66**, 166 (1977).
- (3) F. Dienstbach and F. P. Emmenegger, *Z. Anorg. Allg. Chem.*, in press.
- (4) F. P. Emmenegger, *Inorg. Chem.*, **16**, 343 (1977).
- (5) E. W. Dewing, *Metall. Trans.*, **1**, 2169 (1970).
- (6) A. Dell'Anna and F. P. Emmenegger, *Helv. Chim. Acta*, **58**, 1145 (1975).
- (7) O. Kubaschewski, E. L. Evans and C. B. Alcock, "Metallurgical Thermochemistry", Pergamon Press, Oxford, 1967.
- (8) G. N. Papatheodorou, *J. Phys. Chem.*, **77**, 472 (1973).
- (9) Landolt-Börnstein, "Zahlenwerte und Funktionen", Vol. 2, Springer-Verlag, Heidelberg, 1960.
- (10) H. Schäfer et al., *Z. Anorg. Allg. Chem.*, **278**, 300 (1955).
- (11) The error limit given is twice the standard deviation. Systematic errors are not considered.
- (12) C. W. DeKock and D. R. Gruen, *J. Chem. Phys.*, **44**, 4387 (1966).
- (13) O. N. Komshilova, G. J. Novikov, and O. G. Polyachenok, *Russ. J. Phys. Chem. (Engl. Transl.)*, **43**, 1680 (1969).
- (14) R. Schoonmaker, A. H. Friedmann, and R. F. Porter, *J. Chem. Phys.*, **31**, 1586 (1950).
- (15) H. Schäfer and M. Binnewies, *Z. Anorg. Allg. Chem.*, **410**, 251 (1974).
- (16) R. C. Feber, "Heats of Dissociation of Gaseous Chlorides", Report LA-2841, Los Alamos Scientific Laboratory, 1963; available from the Office of Technical Services, U.S. Department of Commerce, Washington, D.C.
- (17) *Chem. Soc., Spec. Publ.*, No. 17 (1964).

Contribution from the Laboratoire de Chimie de Coordination, 31030 Toulouse Cedex, France, and the Departments of Chemistry, University of Michigan, Ann Arbor, Michigan 48109, and Michigan State University, East Lansing, Michigan 48824

## Microwave Spectrum, Structure, Dipole Moment, and Quadrupole Coupling Constants of Iminosulfur Oxydifluoride

PATRICK CASSOUX,<sup>1a</sup> ROBERT L. KUCZKOWSKI,<sup>\*1b</sup> and ROBERT A. CRESWELL<sup>1c</sup>

Received March 25, 1977

AIC70228K

The microwave spectra of  $\text{HNSOF}_2$ ,  $\text{DNSOF}_2$ ,  $\text{H}^{15}\text{NSOF}_2$ , and  $\text{HN}^{34}\text{SOF}_2$  have been measured. The molecule has a plane of symmetry containing the H, N, S, and O atoms and the hydrogen atom is trans to the oxygen atom. The following structural parameters have been determined from a least-squares analysis of the observed moments of inertia:  $d(\text{NS}) = 1.466 \pm 0.003$  Å,  $d(\text{SO}) = 1.420 \pm 0.005$  Å,  $d(\text{SF}) = 1.549 \pm 0.002$  Å,  $d(\text{NH}) = 1.023 \pm 0.007$  Å,  $\angle\text{NSO} = 119.5 \pm 0.2^\circ$ ,  $\angle\text{NSF} = 112.9 \pm 0.1^\circ$ ,  $\angle\text{FSF} = 93.7 \pm 0.1^\circ$ , and  $\angle\text{HNS} = 115.5 \pm 0.5^\circ$ . The values for the dipole moments obtained from Stark splittings are:  $\text{HNSOF}_2$ ,  $\mu_a = \pm 0.65 \pm 0.01$  D,  $\mu_b = \pm 2.343 \pm 0.005$  D,  $\mu_T = 2.43 \pm 0.01$  D;  $\text{DNSOF}_2$ ,  $\mu_a = \pm 0.45 \pm 0.05$  D,  $\mu_b = \pm 2.44 \pm 0.01$  D,  $\mu_T = 2.48 \pm 0.03$  D. The  $^{14}\text{N}$  quadrupole coupling constants are:  $\text{HNSOF}_2$ ,  $\chi_{aa} = 0.46 \pm 0.02$  MHz,  $\chi_{bb} = 1.75 \pm 0.02$  MHz,  $\chi_{cc} = -2.21 \pm 0.005$  MHz. These data are discussed in terms of the bonding and compared with similar molecules.

### Introduction

Iminosulfur oxydifluoride,  $\text{HN}=\text{S}(\text{O})\text{F}_2$ , was first prepared by Parshall et al.<sup>2</sup> from  $\text{NH}_3$  and  $\text{SOF}_4$  in ether in the presence of NaF. It belongs to the class of sulfur-nitrogen compounds which have been of increasing interest to chemists in recent years and many studies on chemical and physical properties, bonding, and structure have been performed<sup>3</sup> particularly on the acyclic compounds. On the other hand, very few sulfur-nitrogen compounds have been studied by microwave spectroscopy:  $\text{NSF}$ ,<sup>4</sup>  $\text{NSF}_3$ ,<sup>5</sup> *cis*- $\text{HNSO}$ ,<sup>6</sup> and  $\text{NS}$ .<sup>7</sup>

Two of the most interesting questions regarding  $\text{HNSOF}_2$  are the following: (a) the conformation of this molecule (four

possible conformations are shown in Figure 1); (b) the detailed structure, particularly the determination of the N-S bond length, which should provide some insight on the bonding.

Microwave spectroscopy is an excellent tool for studying such problems. In the present work, the microwave spectra of  $\text{HNSOF}_2$ ,  $\text{DNSOF}_2$ ,  $\text{H}^{15}\text{NSOF}_2$ , and  $\text{HN}^{34}\text{SOF}_2$  have been assigned and the structure, dipole moment, and nuclear quadrupole constants were determined.

### Experimental Section

**Synthesis.**<sup>32</sup> The initial sample of the normal species  $\text{HNSOF}_2$ , as well as a sample of  $\text{SOF}_4$  used in the synthesis of the  $^{15}\text{N}$  species,

Table I. Assigned Rotational Transitions and Rotational Constants of HNSOF<sub>2</sub>, DNSOF<sub>2</sub>, H<sup>15</sup>NSOF<sub>2</sub>, and HN<sup>34</sup>SOF<sub>2</sub> (Units are MHz)

Transition	HNSOF <sub>2</sub>	Transition	DNSOF <sub>2</sub>	Transition	H <sup>15</sup> NSOF <sub>2</sub>	Transition	HN <sup>34</sup> SOF <sub>2</sub>
1 <sub>11</sub> -2 <sub>12</sub>	19 109.25 (0.06) <sup>a</sup>	3 <sub>03</sub> -4 <sub>04</sub>	36 760.46 (0.03)	3 <sub>03</sub> -4 <sub>04</sub>	37 425.80 (-0.11)	2 <sub>20</sub> -3 <sub>31</sub>	30 383.85 (0.14)
1 <sub>01</sub> -2 <sub>02</sub>	19 174.19 (0.04)	3 <sub>22</sub> -4 <sub>23</sub>	37 105.64 (0.01)	3 <sub>31</sub> -4 <sub>32</sub>	37 604.75 (-0.08)	2 <sub>21</sub> -3 <sub>30</sub>	30 399.92 (0.04)
1 <sub>10</sub> -2 <sub>11</sub>	19 268.16 (-0.08)	3 <sub>12</sub> -4 <sub>13</sub>	37 334.65 (-0.02)	3 <sub>30</sub> -4 <sub>31</sub>	37 616.65 (-0.04)	3 <sub>22</sub> -4 <sub>13</sub>	37 733.80 (-0.10)
2 <sub>12</sub> -3 <sub>13</sub>	28 655.37 (-0.01)			3 <sub>21</sub> -4 <sub>22</sub>	37 710.10 (-0.02)	3 <sub>13</sub> -4 <sub>04</sub>	38 084.80 (0.24)
2 <sub>02</sub> -3 <sub>03</sub>	28 727.74 (-0.05)	1 <sub>01</sub> -2 <sub>12</sub>	18 675.12 (-0.04)	3 <sub>12</sub> -4 <sub>13</sub>	37 727.25 (-0.04)	3 <sub>03</sub> -4 <sub>14</sub>	38 317.55 (-0.01)
2 <sub>20</sub> -3 <sub>21</sub>	28 838.42 (0.07)	1 <sub>10</sub> -2 <sub>21</sub>	19 567.55 (-0.03)			3 <sub>12</sub> -4 <sub>23</sub>	39 088.42 (-0.16)
		1 <sub>11</sub> -2 <sub>20</sub>	19 802.45 (0.03)	2 <sub>12</sub> -3 <sub>03</sub>	27 844.75 (0.14)	3 <sub>21</sub> -4 <sub>32</sub>	39 941.80 (-0.10)
1 <sub>11</sub> -2 <sub>02</sub>	18 891.76 (-0.05)	2 <sub>21</sub> -3 <sub>12</sub>	27 263.16 (-0.03)	2 <sub>02</sub> -3 <sub>13</sub>	28 295.65 (0.09)		
1 <sub>01</sub> -2 <sub>12</sub>	19 391.66 (0.13)	2 <sub>12</sub> -3 <sub>03</sub>	27 500.84 (0.01)	2 <sub>11</sub> -3 <sub>22</sub>	29 229.55 (0.07)		
1 <sub>10</sub> -2 <sub>21</sub>	20 115.20 (-0.06)	2 <sub>02</sub> -3 <sub>13</sub>	27 730.25 (0.10)	2 <sub>12</sub> -3 <sub>21</sub>	29 604.77 (0.06)		
1 <sub>11</sub> -2 <sub>20</sub>	20 209.36 (0.01)	2 <sub>11</sub> -3 <sub>22</sub>	28 681.95 (-0.10)	2 <sub>20</sub> -3 <sub>31</sub>	30 163.47 (0.08)		
2 <sub>21</sub> -3 <sub>12</sub>	28 045.24 (0.00)	2 <sub>12</sub> -3 <sub>21</sub>	29 471.31 (0.03)	2 <sub>21</sub> -3 <sub>30</sub>	30 183.05 (0.09)		
2 <sub>12</sub> -3 <sub>03</sub>	28 510.35 (-0.06)	2 <sub>20</sub> -3 <sub>31</sub>	29 633.67 (-0.28)	3 <sub>21</sub> -4 <sub>14</sub>	35 772.10 (0.05)		
2 <sub>02</sub> -3 <sub>13</sub>	28 872.83 (0.07)	2 <sub>21</sub> -3 <sub>30</sub>	29 708.93 (0.01)	3 <sub>31</sub> -4 <sub>22</sub>	35 794.69 (0.04)		
2 <sub>11</sub> -3 <sub>22</sub>	29 630.10 (0.01)	3 <sub>13</sub> -4 <sub>04</sub>	36 689.81 (-0.02)	3 <sub>22</sub> -4 <sub>13</sub>	36 812.40 (-0.01)		
2 <sub>12</sub> -3 <sub>31</sub>	29 938.59 (0.07)	3 <sub>22</sub> -4 <sub>13</sub>	36 731.77 (-0.35)	3 <sub>13</sub> -4 <sub>04</sub>	37 244.91 (0.00)		
2 <sub>20</sub> -3 <sub>31</sub>	30 387.03 (0.40)	3 <sub>03</sub> -4 <sub>14</sub>	36 786.41 (0.01)	3 <sub>12</sub> -4 <sub>23</sub>	38 476.03 (-0.08)		
2 <sub>21</sub> -3 <sub>30</sub>	30 403.65 (-0.04)			3 <sub>13</sub> -4 <sub>22</sub>	39 289.22 (0.00)		
3 <sub>21</sub> -4 <sub>14</sub>	36 910.52 (0.01)			3 <sub>21</sub> -4 <sub>32</sub>	39 520.10 (-0.10)		
3 <sub>12</sub> -4 <sub>23</sub>	39 103.77 (-0.07)			3 <sub>22</sub> -4 <sub>31</sub>	39 618.38 (-0.03)		
3 <sub>13</sub> -4 <sub>22</sub>	39 772.20 (-0.11)						
	A = 5119.28 ± 0.01		A = 5003.45 ± 0.01		A = 5094.79 ± 0.01		A = 5119.10 ± 0.05
	B = 4836.94 ± 0.01		B = 4731.34 ± 0.01		B = 4745.38 ± 0.01		B = 4834.14 ± 0.05
	C = 4757.42 ± 0.01		C = 4557.24 ± 0.01		C = 4648.37 ± 0.01		C = 4754.48 ± 0.05

<sup>a</sup> Numbers in parentheses are  $\nu_{\text{obsd}} - \nu_{\text{calcd}}$ .

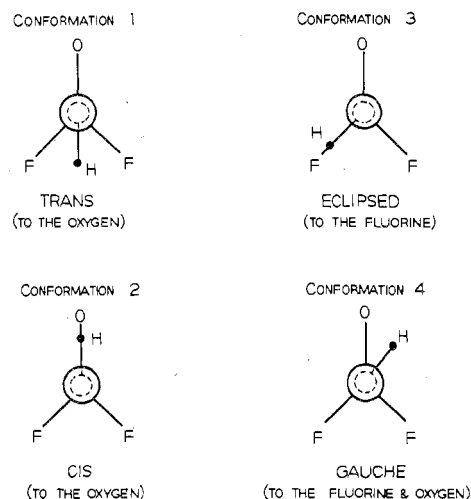


Figure 1. Possible conformations of HNSOF<sub>2</sub>.

was kindly supplied by O. Glemser.

DNSOF<sub>2</sub> was prepared in about 60% enrichment by exchange of HNSOF<sub>2</sub> with D<sub>2</sub>O in the presence of traces of HCl (identification by IR spectroscopy;  $\nu_{\text{ND}} = 2540 \text{ cm}^{-1}$ ).

H<sup>15</sup>NSOF<sub>2</sub> was prepared following Parshall's procedure.<sup>2</sup> The reaction is preferably run in diethyl ether and the immediate product is an azeotrope from which H<sup>15</sup>NSOF<sub>2</sub> can be distilled following addition of BF<sub>3</sub> to neutralize the ether. However, as our synthesis had to be scaled down (0.38 g of <sup>15</sup>NH<sub>3</sub> as starting material) careful microdistillation yielded a fraction boiling at maximum 40 °C (about 20% H<sup>15</sup>NSOF<sub>2</sub>). Another complication was the addition of BF<sub>3</sub> since it complexed with HNSOF<sub>2</sub> as well as the ether. Purification by preparative gas chromatography was unsuccessful because of the low boiling point of the compound (43 °C). H<sup>15</sup>NSOF<sub>2</sub> was identified in the mixture by IR spectroscopy ( $\nu^{15}\text{NH} = 3420 \text{ cm}^{-1}$ ) and NMR (<sup>1</sup>H,  $\tau$  ppm/TMS = 11.4; <sup>19</sup>F,  $\phi$  ppm/CF<sub>3</sub>COOH = 134). The sample used for measurements contained about 20% of H<sup>15</sup>NSOF<sub>2</sub>.

**Spectrometers.** Most microwave spectra were obtained with a 80-kHz square-wave modulated spectrometer of conventional design.<sup>8</sup> Some spectra were acquired using a Hewlett-Packard Model 8460A spectrometer.<sup>9</sup> In general, frequency measurements had an accuracy of better than ±0.10 MHz. The <sup>14</sup>N quadrupole splittings of some transitions were measured with an accuracy of ±0.01 MHz. The sample cell was cooled to dry ice temperature.

## Results and Analysis

**Microwave Spectrum of HNSOF<sub>2</sub>.** The 20 *a* and *b* type rotational transitions observed for the normal species are listed in Table I. These were principally assigned on the basis of their Stark effects and fitted to a rigid rotor model with the calculated rotational constants also listed in Table I. The assignment was later confirmed by measurement of the <sup>14</sup>N quadrupole splittings of some transitions.

However, some particular features of this rich and intense spectrum were initially confusing. The first difficulty was caused by our expectation, based on initial structural guesses, that transitions with *a* and *c* type selection rules would be found. Instead, we later realized that *a* and *b* type transitions were being observed. This resulted because HNSOF<sub>2</sub>, as will be shown again in the structure analysis, is a near spherical top and small changes in structural parameters have a large effect on the orientation of the principal axes.

Another complication was the presence of dense regions of very strong lines which made it more difficult to observe some weaker low *J* lines. These regions were identified as Q branch series. The spacing between two band heads is about 640 MHz, which corresponds roughly to the quantity  $2A - B - C$  (644.2 MHz).

For some transitions (e.g., 2<sub>21</sub> → 3<sub>12</sub> and 2<sub>21</sub> → 3<sub>30</sub>) the observed Stark effect pattern was not consistent with the Stark coefficients calculated by second-order perturbation theory for *M* ≠ 0 transitions.<sup>10</sup> This inconsistency arose from the near degeneracy of some *K<sub>a</sub>* doublets (e.g., the 2<sub>20</sub> and 2<sub>21</sub> levels). In such cases, qualitative agreement with the observed Stark effect could be obtained by diagonalization of the complete Stark energy matrix.<sup>11</sup>

In some other cases, surprisingly strong Stark components were observed, while the corresponding zero-field lines were absent. These transitions arise from the mixing of the wave functions of the interacting near degenerate *K<sub>a</sub>* doublets so that *c*-type transitions forbidden in the absence of the Stark field became allowed when the field was turned on. The hypothetical zero-field frequencies of these lines were approximately determined either by extrapolation of the frequency of the Stark components as a function of the square of the field or when this function was not linear, by measuring the fre-

Table II. Frequencies of Forbidden *c*-Type Transitions

Species	Transition	$\nu_{\text{obsd}},^a$ MHz	$\nu_{\text{calcd}},$ MHz
HNSOF <sub>2</sub>	1 <sub>10</sub> -2 <sub>20</sub>	20 129.7	20 129.83
	1 <sub>11</sub> -2 <sub>21</sub>	20 194.3	20 194.79
	2 <sub>20</sub> -3 <sub>30</sub>	30 389.4	30 389.13
	2 <sub>21</sub> -3 <sub>31</sub>	30 401.6	30 401.99
DNSOF <sub>2</sub>	2 <sub>20</sub> -3 <sub>30</sub>	29 648.6	29 648.19
	2 <sub>21</sub> -3 <sub>31</sub>	29 694.1	29 694.68

<sup>a</sup> Hypothetical zero-field frequencies obtained by extrapolation. Cf. text.

quency of the Stark component at the lowest possible field. As shown in Table II, the frequencies of these hypothetical zero-field lines were found to be very close to those of *c*-type transitions calculated on the basis of the rotational constants of Table I.

**Microwave Spectrum of DNSOF<sub>2</sub>.** The assignment of the spectrum of DNSOF<sub>2</sub> was based upon the Stark effect, the rigid rotor fit, and the expected isotope shift. The frequencies of 16 *a* and *b* type transitions are listed in Table I. The calculated rotational constants are also given in Table I.

Particular features, similar to those of the spectrum of HNSOF<sub>2</sub>, were also observed in the spectrum of DNSOF<sub>2</sub>: (i) the presence of Q branch series (spacing between two band heads  $\approx$  800 MHz), (ii) the Stark effect of some lines inconsistent with those calculated by second-order perturbation theory, and (iii) the presence of Stark components originating from forbidden *c*-type transitions (Table II).

**Microwave Spectrum of H<sup>15</sup>NSOF<sub>2</sub>.** The assigned transitions for H<sup>15</sup>NSOF<sub>2</sub> are listed in Table I together with the calculated rotational constants. The Q branch transitions were relatively less intense (spacing  $\approx$  730 MHz). As this spectrum was readily assigned on the basis of the frequency fit and expected isotope shifts no further consideration was given to non-second-order Stark effects or forbidden *c*-type transitions.

**Microwave Spectrum of HN<sup>34</sup>SOF<sub>2</sub>.** Seven *b*-type rotational transitions were observed for the <sup>34</sup>S species in natural abundance and are listed in Table I. These transitions were identified by their intensities, the temperature dependence of the intensities, Stark effects, and frequency fit. In no case could an alternative transition be assigned which had all the proper characteristics and which occurred within 25 MHz of the assigned transition. Three of these transitions were also measured using the rf-microwave double-resonance technique. The uncertainty in the frequency measurements for these weaker transitions was about  $\pm 0.2$  MHz.

**Structure.** Information about the conformation can be obtained by noting the similar value for  $I_a + I_b - I_c$  for the four isotopic species (Table III). From this it is concluded that HNSOF<sub>2</sub> has a plane of symmetry containing the H, N, S, and O atoms and the *a* and *b* principal axes. *Gauche* conformations 3 and 4 of Figure 1 can thus be ruled out. This is also confirmed by the absence of any allowed *c*-type transitions and by the measurements of the dipole moments (cf. Dipole Moments subsection).

The *a* and *b* coordinates of the hydrogen, nitrogen, and sulfur atoms can be calculated using the Kraitchman equations.<sup>12</sup> These  $r_s$  coordinates are listed in Table III. The uncertainty in the nitrogen and sulfur coordinates are those based on experimental uncertainties in *A*, *B*, and *C*. For hydrogen, different  $r_s$  values are obtained depending on whether  $\Delta I_a + \Delta I_b - \Delta I_c$  is set to zero or equal to the experimental value of  $0.048 \text{ u } \text{\AA}^2$ ; the hydrogen  $r_s$  value listed in Table III is the average of these values with an uncertainty sufficient to include the range plus experimental uncertainty. It is obvious from the magnitudes of the coordinates that both N and H are located in the same *ab* quadrant which leads to  $d(\text{NH}) = 1.023 \pm 0.007 \text{ \AA}$ . Likewise, upon considering

Table III. Kraitchman Coordinates and Planar Second Moments

Atom	Coordinate, A	Species	$I_a + I_b - I_c,^a \text{ u } \text{\AA}^2$
H	$ a  = 1.190 \pm 0.0010$	HNSOF <sub>2</sub>	96.973
	$ b  = 1.813 \pm 0.0070$	DNSOF <sub>2</sub>	96.925
N	$ a  = 1.369 \pm 0.0001$	H <sup>15</sup> NSOF <sub>2</sub>	96.972
	$ b  = 0.806 \pm 0.0002$	HN <sup>34</sup> SOF <sub>2</sub>	96.972
S	$ a  = 0.176 \pm 0.0014$		
	$ b  = 0.047 \pm 0.0050$		

<sup>a</sup> Conversion factor  $505 \text{ 376 MHz u } \text{\AA}^2$ .

possible signs for F and O it becomes apparent from calculations using the first moment and cross product condition,  $I_{ab} = 0$ , that the *a* coordinates of N and S have the same sign while their *b* coordinates have opposite signs (this is also confirmed by the least-squares analysis of the observed moments of inertia). This leads to  $d(\text{NS}) = 1.466 \pm 0.003 \text{ \AA}$  and  $\angle \text{HNS} = 115.5 \pm 0.5^\circ$ . The *c* coordinate of the out-of-plane fluorine atoms can also be obtained directly from the relation  $I_a + I_b - I_c = 4m_F c_F^2$ , giving  $c_F = \pm 1.1295 \pm 0.0001 \text{ \AA}$ .

Before discussing the determination of the remaining structural parameters, it is interesting to point out the reasoning that was required to arrive at the correct conformation and a unique structure. In the earlier stages of this work, four models were obtained which fitted the experimental rotational constants of HNSOF<sub>2</sub> and DNSOF<sub>2</sub>. Two plausible *trans* (to the oxygen atom) conformers were found with the orientation of the *a* and *b* axes interchanged. Two *cis* conformers were likewise found.<sup>13</sup> This reflects the near spherical top character of the structure of HNSOF<sub>2</sub> for which small changes in the geometrical parameters (two of them had to be assumed) have a large effect on the orientation of the principal axes. One *cis* and one *trans* model were later ruled out on the basis of the <sup>15</sup>N data, but an unequivocal solution to the problem was still not obtained at this point. However, the remaining possible *cis* model contained some bond angles substantially different from the corresponding values in related molecules such as CINSOF<sub>2</sub>, SO<sub>2</sub>F<sub>2</sub>, HNSO, and CINSF<sub>2</sub> and seemed less plausible. By contrast the bond angles for the remaining *trans* model were all close to those observed in the related molecules. These two models predicted sufficiently distinct <sup>34</sup>S isotope shifts and they finally led to the assignment of the <sup>34</sup>S transitions for the remaining *trans* model and an unambiguous conformational determination.

The remaining structural parameters were determined by least-squares fitting of the experimental moments of inertia, the nontrivial center-of-mass and product-of-inertia relations.<sup>14</sup> Two strategies were employed. (1) The Kraitchman coordinates and  $c_F$  of Table III were held constant while the remaining coordinates were adjusted; in that case, the uncertainties in the Kraitchman coordinates were also propagated through the calculation. (2) All the moments of inertia were fit without using the Kraitchman coordinates; the difference between the adjusted coordinates of N, H, and S and the corresponding Kraitchman coordinates was found to be less than  $0.01 \text{ \AA}$ .

The parameters derived from these two strategies agreed within  $0.005 \text{ \AA}$  and  $0.5^\circ$ . This indicates that the mixed  $r_s, r_o$  structure (strategy 1) is not very different from the  $r_o$  structure (strategy 2). A further implication is that no unusual problems from small coordinates, large axes rotations upon substitution, or unusual vibrational effects seem to complicate seriously the structure determination. In fact the calculated rotational constants agree with the experimental values to better than  $0.1 \text{ MHz}$  and the root-mean-square deviation of the moments fitted was smaller than  $0.005 \text{ u } \text{\AA}^2$ .

Table IV. Structural Parameters<sup>a</sup> of HNSOF<sub>2</sub> and Related Molecules

Parameter	HNSOF <sub>2</sub> <sup>c</sup>	CIN-SOF <sub>2</sub> <sup>d</sup>	SO <sub>2</sub> -F <sub>2</sub> <sup>e</sup>	HNSO <sup>f</sup>	CIN-SF <sub>2</sub> <sup>g</sup>
<i>d</i> (NS)	1.466 ± 0.003 <sup>b</sup>	1.484		1.512	1.476
<i>d</i> (SO)	1.420 ± 0.005	1.394	1.405	1.451	
<i>d</i> (SF)	1.549 ± 0.002	1.548	1.530		1.596
<i>d</i> (NH)	1.023 ± 0.007			1.029	
∠NSO	119.5 ± 0.2	117.4		120.4	
∠NSF	112.9 ± 0.1	111.8			111.2
∠FSF	93.7 ± 0.1	92.6	96.1		89.8
∠HNS	115.5 ± 0.5			115.8	

<sup>a</sup> Bond lengths are in Å units, bond angles in deg. <sup>b</sup> Uncertainties from experimental rotational constants. Overall uncertainties of ±0.01 Å and ±0.5° are estimated for vibrational effects and should encompass the average structure. <sup>c</sup> This work. <sup>d</sup> Reference 16. <sup>e</sup> Reference 17. <sup>f</sup> Reference 6. <sup>g</sup> Reference 18.

Table V. Some Observed NS Bond Lengths and NS Bond Orders

Molecule	<i>d</i> (NS), Å	<i>N</i> <sub>NS</sub> <sup>a</sup>
NSF <sub>3</sub>	1.416 <sup>4</sup>	2.7
NSF	1.446 <sup>3</sup>	2.4
HNSOF <sub>2</sub>	1.466, this work	(≈2.2) <sup>b</sup>
CINSF <sub>2</sub>	1.476 <sup>18</sup>	(≈2.1)
CINSOF <sub>2</sub>	1.484 <sup>16</sup>	(≈2.0)
NS	1.494 <sup>7</sup>	(≈1.9)
<i>cis</i> -HNSO	1.512 <sup>6</sup>	1.9
N <sub>2</sub> S <sub>4</sub>	1.63 <sup>19</sup>	1.2
NH <sub>2</sub> SO <sub>3</sub> H	1.73 <sup>20</sup>	0.8

<sup>a</sup> *N*<sub>NS</sub> is the nitrogen-sulfur bond order discussed in text and in ref 3. <sup>b</sup> Numbers in parentheses are the interpolated NS bond orders.

The result of the structure determination from strategy 1 is summarized in Table IV. The uncertainty limits are based on the experimental uncertainty in the rotational constants. There is an additional uncertainty arising from vibrational effects which is more difficult to estimate. From the close correspondence for the two methods of calculation, it seems reasonable to expect the structural parameters with attached uncertainties of ±0.01 Å and ±0.5° to encompass the well-defined average structure.<sup>15</sup>

Table IV also contains a comparison of the structural parameters with those in related molecules. A particularly interesting comparison involves the NS bond length which is listed in Table V together with the corresponding *N*<sub>NS</sub> bond orders estimated by Glemser.<sup>3</sup> The NS bond length in HNSOF<sub>2</sub> is one of the shortest observed for such compounds and its bond order may be approximately interpolated to a value close to 2.2. It may be noted that in HNSOF<sub>2</sub> *d*(NS) is about 0.04 Å shorter and *d*(SO) is also shorter by about 0.03 Å than in *cis*-HNSO, and the bond multiplicities are presumably higher.<sup>21</sup> This shortening has a parallel observation in phosphorus compounds. A well-documented, systematic decrease in bond distances to phosphorus is observed as the electronegativity of the bonded groups increases and as the coordination number of phosphorus increases.<sup>22,23</sup>

**Dipole Moments.** The electric dipole moment of HNSOF<sub>2</sub> was calculated from the measurements of the *M* = 0 components of eight transitions. These components were observed to have a second-order Stark effect. The Stark coefficients were calculated using the method of Golden and Wilson.<sup>10</sup> The electric field was calibrated by using the *J* = 2 ← 1 transition of OCS.<sup>24</sup> The fit of the observed Stark coefficients to three dipole moment components leads to low positive (0.03 D<sup>2</sup>) or even negative values for  $\mu_c$  with large uncertainties. This again indicates the HNSOF<sub>2</sub> has a plane of symmetry. For the final dipole moments calculation  $\mu_c$  was set equal to zero. The calculated and measured Stark coefficients are listed in Table VI along with the values of the dipole moment com-

Table VI. Stark Coefficients (MHz cm<sup>2</sup> 10<sup>5</sup>/V<sup>2</sup>) and Dipole Moment (D) of HNSOF<sub>2</sub> and DNSOF<sub>2</sub> (*M*=0 Components)

Transition	HNSOF <sub>2</sub>		DNSOF <sub>2</sub>	
	Obsd	Calcd	Obsd	Calcd
1 <sub>11</sub> -2 <sub>02</sub>	-2.863	-2.849		
1 <sub>10</sub> -2 <sub>21</sub>	+1.773	+1.772		
1 <sub>11</sub> -2 <sub>20</sub>	-2.552	-2.556	-2.937	-3.032
2 <sub>21</sub> -3 <sub>12</sub>	-0.585	-0.585		
2 <sub>12</sub> -3 <sub>03</sub>	-0.358	-0.357		
2 <sub>11</sub> -3 <sub>22</sub>	+0.642	+0.644		
2 <sub>12</sub> -3 <sub>21</sub>	-0.507	-0.507	-0.655	-0.653
2 <sub>21</sub> -3 <sub>30</sub>	-0.139	-0.138	-0.199	-0.202
1 <sub>01</sub> -2 <sub>12</sub>			1.958	1.899
2 <sub>02</sub> -3 <sub>13</sub>			0.244	0.241
$ \mu_a $	0.65 ± 0.01		0.45 ± 0.05	
$ \mu_b $	2.343 ± 0.005		2.44 ± 0.01	
$\mu_{total}$	2.43 ± 0.01		2.48 ± 0.03	

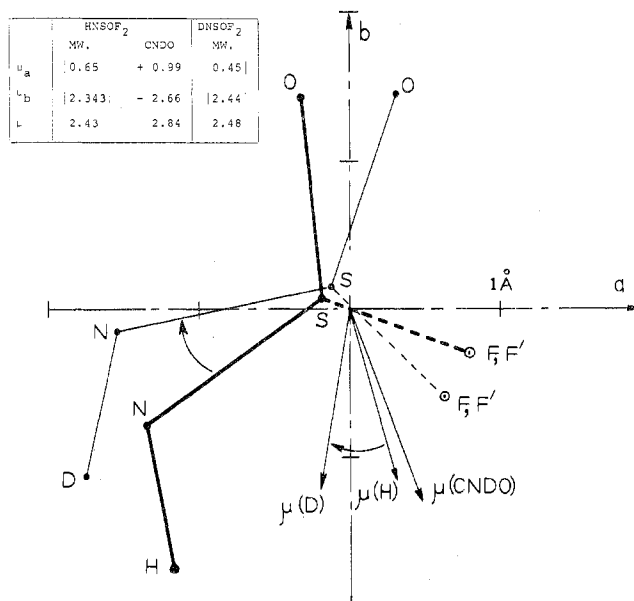


Figure 2. Projections of atom coordinates for HNSOF<sub>2</sub> and DNSOF<sub>2</sub> and orientations of their molecular dipole moments in the *ab* principal axes plane.

ponents from the least-squares fit.

The dipole moment of DNSOF<sub>2</sub> was also calculated from the measurements of five *M* = 0 components. The calculated and measured Stark coefficients and the dipole moment components are also listed in Table VI.

The effect of deuterium substitution on the magnitude of the  $\mu_a$  and  $\mu_b$  components indicates that the total dipole moment is oriented approximately parallel to the SO bond direction. However, it is difficult to infer by a simple appeal to electronegativities or bond moments if the negative direction is pointed toward the oxygen or away from it. Therefore, semiempirical MO calculations (CNDO/2)<sup>25</sup> were carried out. The calculated  $\mu_a$  and  $\mu_b$  components compare well with the absolute values of the experimental components, as shown in Figure 2. Guided by the signs for the theoretically calculated dipole components, the orientation of the experimental dipole moments depicted in Figure 2 was selected with the arrowhead indicating the negative direction.<sup>26</sup>

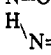
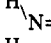
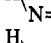
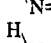
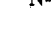
**<sup>14</sup>N Quadrupole Coupling Constants.** For some transitions, hyperfine structure due to the <sup>14</sup>N electric quadrupole was observed at low pressures. The quadrupole splittings of the  $\Delta F = 1$  components of six transitions of HNSOF<sub>2</sub> are listed in Table VII. These components were assigned on the basis of their relative intensity and fitted to the calculated quadrupole constants  $\chi_{aa}$ ,  $\chi_{bb}$ , and  $\chi_{cc}$ , which are listed in Table

Table VII. Calculated and Observed Quadrupole Hyperfine Structure in HNSOF<sub>2</sub>

Transition	F → F'	$\nu_{\text{obsd}}$	$\nu_{\text{obsd}} - \nu_{\text{calcd}}$	$\nu_0$
1 <sub>11</sub> -2 <sub>02</sub>	2-3	18 891.852	-0.024	18 891.854
	1-2	18 891.659	+0.009	
	0-1	18 892.511	+0.015	
2 <sub>11</sub> -3 <sub>22</sub>	3-4	29 629.880	-0.008	29 630.013
	2-3	29 630.451	+0.001	
	1-2	29 629.583	+0.007	
2 <sub>12</sub> -3 <sub>21</sub>	3-4	29 938.734	+0.005	29 938.481
	2-3	29 937.661	+0.002	
	1-2	29 939.242	-0.007	
3 <sub>21</sub> -4 <sub>14</sub>	4-5	36 909.970	-0.017	36 910.319
	3-4	36 911.258	+0.001	
	2-3	36 909.642	+0.015	
3 <sub>13</sub> -4 <sub>22</sub>	4-5	39 772.480	+0.020	39 772.130
	3-4	39 771.160	-0.012	
	2-3	39 772.860	-0.007	
3 <sub>12</sub> -4 <sub>23</sub>	4-5	39 103.430	-0.003	39 103.581
	3-4	39 104.010	+0.010	
	2-3	39 103.250	-0.014	

$\chi_{aa} = 0.46 \pm 0.02$  MHz  
 $\chi_{bb} = 1.75 \pm 0.02$  MHz  
 $\chi_{cc} = -2.21 \pm 0.005$  MHz

Table VIII. Comparison of Out-of-Plane <sup>14</sup>N Nuclear Quadrupole Coupling for NO and Compounds with Imine Group

Molecule	$\chi_{cc}$ , MHz	$(U_p)_c$	N=X bond length	Ref
N=O	0.92 <sup>a</sup>	0.092 <sup>b</sup>	1.15	27
	5.10	0.510	1.212	28
	3.55	0.355	1.273	29
	-1.583	-0.158	1.207	30
	1.57	0.157	1.512	6
	-2.21	-0.221	1.466	This work

<sup>a</sup> This is the coupling constant perpendicular to the bond axis; calculated with Laplace's theorem. <sup>b</sup> See text for definition of  $(U_p)_c$ .

VII along with the theoretical unsplit frequencies ( $\nu_0$ ).

It is interesting to compare the <sup>14</sup>N quadrupole constant of HNSOF<sub>2</sub> perpendicular to the symmetry plane with that obtained by Kirchhoff for the related molecule *cis*-HNSO.<sup>6</sup> The bonding around the nitrogen atom should be very similar in both molecules if the angle HNS is used as a guide since it is nearly identical in the two compounds. However, the out-of-plane constant  $\chi_{cc}$  of HNSOF<sub>2</sub> (-2.21 MHz) is very different from  $\chi_{cc}$  of *cis*-HNSO (1.57 MHz) and consequently the charge distribution near the nitrogen atom is considerably different in the two compounds. Other evidence for this is the NS bond length which is shorter by 0.05 Å in HNSOF<sub>2</sub>.

A similar trend for the out-of-plane coupling constant and bond length is also observed for HN=CH<sub>2</sub> vs. HN=C=O and HN=O vs. N=O (Table VIII). It is attractive to correlate the decrease in  $\chi_{cc}$  and  $d(\text{N}=\text{X})$  with increased importance of  $\pi$  bonding. Support for this correlation is obtained upon application of the simple formula discussed by Gordy and Cook.<sup>31</sup>

$$\chi_{zz} = -(U_p)_z e q Q_{n10}$$

In this case  $\chi_{zz}$  is the out-of-plane coupling constant ( $\chi_{cc}$ ) and  $e q Q_{n10}$  is the quadrupole coupling constant due to one electron in a p orbital. For nitrogen,  $e q Q_{210}$  is usually estimated as -10

MHz.  $(U_p)_z = (n_x + n_y)/2 - n_z$  and represents the unbalanced p electrons in the z direction. A positive  $(U_p)_z$  corresponds to a p electron deficit in the z direction and vice versa. It can be seen in Table VIII that HNCO and HNSOF<sub>2</sub> have an electron excess out of the plane. This is presumably an indication of increased  $\pi$  bonding in these compounds, which correlates readily with their shorter bond lengths. This conclusion is supported by the calculated values of  $(U_p)_c$  by CNDO/2 for HNSOF<sub>2</sub> (-0.33) and *cis*-HNSO (0.03) which compare fairly well with the values extracted from the microwave data (-0.22 and 0.16, respectively).

**Acknowledgment.** The authors are grateful to the NATO Scientific Affairs Division for the support of this work (Research Grant No. 925). The work was also supported by grants from the National Science Foundation to the University of Michigan (GP-38750X1 and CHE 76-09572) and to Michigan State University (CHE 74-21841) and by the NSF-CNRS Scientist Exchange Program (U.S.-France). We wish to thank O. Glemser who originally directed our attention to this problem and provided us with a sample of HNSOF<sub>2</sub> and SOF<sub>4</sub>. We are also indebted to Dr. G. Parshall who provided a sample of SOF<sub>4</sub>, to Professor L. S. Bartell for help and discussions on the structural analysis and to Professor R. H. Schwendeman for discussions on various aspects of this work and use of computer programs. The helpful assistance by F. Sournies is acknowledged.

Registry No. HNSOF<sub>2</sub>, 20994-96-1; DNSOF<sub>2</sub>, 63848-86-2; H<sup>15</sup>NSOF<sub>2</sub>, 63848-85-1; HN<sup>14</sup>SOF<sub>2</sub>, 63848-84-0.

## References and Notes

- (a) Laboratoire de Chimie de Coordination; (b) University of Michigan; (c) Michigan State University.
- G. W. Parshall, R. Cramer, and R. E. Foster, *Inorg. Chem.*, **1**, 677 (1962).
- Cf., for example, the general review: O. Glemser and R. Mews, *Adv. Inorg. Chem. Radiochem.*, **14**, 333 (1972).
- W. H. Kirchhoff and E. B. Wilson, *J. Am. Chem. Soc.*, **85**, 1726 (1963); R. L. Cook and W. H. Kirchhoff, *J. Chem. Phys.*, **47**, 4521 (1967); A. M. Mirri and A. Guarnieri, *Spectrochim. Acta, Part A*, **23a**, 2159 (1967).
- W. H. Kirchhoff and E. B. Wilson, *J. Am. Chem. Soc.*, **84**, 334 (1962).
- W. H. Kirchhoff, *J. Am. Chem. Soc.*, **91**, 2437 (1969).
- T. Amano, S. Saito, E. Hirota, and Y. Morino, *J. Mol. Spectrosc.*, **32**, 97 (1969).
- R. L. Kuczkowski, *J. Am. Chem. Soc.*, **90**, 1705 (1968).
- D. R. Johnson and R. Pearson, Jr., "Methods of Experimental Physics", Vol. 13, Part B, Academic Press, New York, N.Y., 1976.
- S. Golden and E. B. Wilson, Jr., *J. Chem. Phys.*, **16**, 669 (1948); the program we have used was written by R. A. Beaudet.
- J. Kraitchman and B. P. Dailey, *J. Chem. Phys.*, **23**, 184 (1955); the program we have used was written by R. H. Schwendeman.
- J. Kraitchman, *Am. J. Phys.*, **21**, 17 (1953).
- Assistance in identifying these four possibilities was obtained by using the "Method of Predicate Observations", L. S. Bartell, D. J. Romensko and T. C. Wong, *Mol. Struct. Diffr. Methods*, **3**, (1975); and personal communication.
- Program STRFIT written by R. H. Schwendeman was used; R. H. Schwendeman, "Critical Evaluation of Chemical and Physical Structural Information", National Academy of Sciences, Washington, D.C., 1974.
- V. Laurie and D. Herschbach, *J. Chem. Phys.*, **37**, 1668 (1962).
- O. Oberhammer, O. Glemser, and H. Klüver, *Z. Naturforsch. A*, **29**, 901 (1974).
- D. R. Lide, Jr., D. E. Mann, and R. M. Fristom, *J. Chem. Phys.*, **26**, 734 (1957).
- J. Haase, H. Oberhammer, W. Zeil, O. Glemser, and R. Mews, *Z. Naturforsch. A*, **25**, 153 (1970).
- C. S. Lu and J. Donohue, *J. Am. Chem. Soc.*, **66**, 818 (1944); B. D. Sharma and J. Donohue, *Acta Crystallogr.*, **16**, 891 (1963).
- F. A. Kanda and A. J. King, *J. Am. Chem. Soc.*, **73**, 2315 (1951).
- trans*-HNSO also exists but is less stable than *cis*-HNSO and detailed structural data are not available: P. O. Tchir and R. D. Spratley, *Can. J. Chem.*, **53**, 2331 (1975).
- P. S. Bryan and R. L. Kuczkowski, *Inorg. Chem.*, **11**, 553 (1972).
- Y. Morino, K. Kuchitsu, and T. Moritani, *Inorg. Chem.*, **8**, 867 (1969).
- J. S. Muentner, *J. Chem. Phys.*, **48**, 4544 (1968).
- J. A. Pople and D. L. Beveridge, "Approximate Molecular Orbital Theory", McGraw-Hill, New York, N.Y., 1970.
- Ab initio MO calculations have also confirmed this direction: P. C. Cassoux and A. Serafini, unpublished study.
- W. L. Meerts and A. Dymanus, *J. Mol. Spectrosc.*, **44**, 320 (1972).
- S. Saito and K. Tatagi, *J. Mol. Spectrosc.*, **47**, 99 (1973).

- (29) D. R. Johnson and F. J. Lovas, *Chem. Phys. Lett.*, **15**, 65 (1972); R. Pearson and F. J. Lovas, Abstracts, 31st Symposium on Molecular Spectroscopy, Columbus, Ohio, June, 1976.  
 (30) W. H. Hocking, M. C. L. Gerry, and G. Winnewisser, *Can. J. Phys.*,

- 53**, 1869 (1975).  
 (31) W. Gordy and R. L. Cook, "Microwave Molecular Spectra", Interscience, New York, N.Y., 1970, Chapter 14.  
 (32) Technical assistance by F. Sournies.

## Notes

Contribution from the Department of Chemistry,  
 University of Vermont, Burlington, Vermont 05401

### Reactions of Hexafluorocyclotriphosphazene with Lithium Enolate Anions

John G. DuPont and Christopher W. Allen\*

Received January 24, 1977

AIC70061V

In recent years, the reactions of hexafluorocyclotriphosphazene ( $P_3N_3F_6$ ) with alkyl-<sup>1</sup>, alkynyl-<sup>2</sup>, and aryllithium<sup>3,4</sup> reagents have been investigated. Thus, many compounds not available by direct synthesis<sup>5</sup> or the Friedel-Crafts reaction<sup>5</sup> may be prepared. In view of the fact that lithium enolate anions of ketones are known to react as nucleophilic reagents,<sup>6</sup> it would appear to be worthwhile to attempt reactions of these species with  $P_3N_3F_6$ . If successful, these reactions would yield phosphazenes with a ketone function in the exocyclic group which would be the precursors of a wide variety of organocyclophosphazenes derived from reactions of the carbonyl group. Therefore, we wish to report the synthesis and characterization of the pentafluorocyclotriphosphazene derivatives of acetophenone (I,  $P_3N_3F_5CH_2C(O)C_6H_5$ ) and cyclohexanone (II,  $P_3N_3F_5C_6H_9O$ ).

### Experimental Section

All reactions were carried out under anhydrous conditions and a nitrogen atmosphere. Diethyl ether and tetrahydrofuran were distilled from sodium/benzophenone. Hexafluorocyclotriphosphazene was prepared from hexachlorocyclotriphosphazene (El monte or Ethyl Corp.) by previously established procedures.<sup>7</sup> Diisopropylamine was purified by distillation over calcium hydride. Commercially available *n*-butyllithium, acetophenone, and cyclohexanone were used without further purification. NMR spectra (in  $CDCl_3$ ) were obtained on a JEOL C60-HL spectrophotometer at 60 MHz (<sup>1</sup>H) or 56.5 MHz (<sup>19</sup>F). Tetramethylsilane (<sup>1</sup>H) and fluorotrichloromethane (<sup>19</sup>F) were used as internal standards. Infrared spectra were obtained on thin films using a Beckman IR-20A spectrophotometer with sodium chloride or polyethylene disks. Mass spectra were obtained on a Perkin-Elmer RMU-6D spectrometer operating at 80 eV. Samples were introduced through the liquid inlet. Analytical samples were purified by preparative-layer chromatography (silica/pentane) or preparative VPC using a Gow Mac 69-100 chromatography equipped with a DC 200 Chromsorb column. Elemental analyses were performed by Robertson Laboratories.

**Preparation of  $P_3N_3F_5CH_2C(O)C_6H_5$  (I).** To a stirred solution of 5.1 g (0.05 mol) of diisopropylamine in 20 mL of tetrahydrofuran (THF)<sup>8</sup> at -78 °C was added 21 mL of *n*-butyllithium in hexane (0.048 mol). After stirring for 20 min, 6.0 g (0.05 mol) of acetophenone in 20 mL of THF was added dropwise over a 1-h period.<sup>6</sup> After an additional hour of stirring, the solution was allowed to reach room temperature and was added dropwise to a stirred solution of 12.5 g (0.05 mol) of  $P_3N_3F_6$  in 50 mL of THF. The clear solution gradually turned to a vivid yellow and finally a pale orange after 3 h under refluxing conditions. The solvent was removed under aspirator vacuum and the remaining oil was dissolved in diethyl ether and extracted with acidified water. Evaporation of the ether layer yielded a brown oil which was then distilled at 75–80 °C and 4–5 mmHg to give 8.45 g (48% of theory) of a water white oil. VPC analysis of the distillate showed it to be a 95/5 mixture of  $P_3N_3F_5CH_2C(O)C_6H_5$  and acetophenone. Analytical sample purification was done by either preparative-layer chromatography or preparative VPC. Anal. Calcd

for  $P_3N_3F_5C_8H_7O$ : C, 27.51; H, 2.01; mol wt 350. Found: C, 27.63; H, 2.19; mol wt 350 (mass spectrum).

NMR:<sup>9</sup> <sup>19</sup>F  $\delta$ (PF<sub>2</sub>) 62.0 (4 F,  $J$ (PF) = 788 Hz),  $\delta$ (PFR) 58.0 (1 F,  $J$ (PF) = 778 Hz); <sup>1</sup>H  $\delta$ (CH<sub>2</sub>) 5.4 (2 H,  $J$ (PH) = 15 Hz),  $\delta$ (C<sub>6</sub>H<sub>5</sub>) 7.5 (5 H). IR:<sup>10</sup> 3020 (m, CH str), 2950 (w, CH str), 1640 (s, CO str), 1580 (m, CC str), 1490 (m, CC str), 1450 (m, CH bend), 1270 (s, PN str), 1080 (s, PN<sup>1</sup> str), 1050 (m, CH bend), 1010 (m, CH bend), 980 (s, PF asym), 890 (s), 950 (s, PF sym), 840 (s, PF sym), 760 (s, PF sym), 740 (m), 700 (s), 670 (m), 580 (w), 570 (w), 560 (w), 500 (s), 450 (s). Mass spectra:<sup>11</sup> 350 (100%,  $P_3N_3F_5C_8H_7O^+$ ), 334 (6%,  $P_3N_3F_5C_8H_7^+$ ), 247 (21%,  $P_3N_3F_5OH^+$ ), 244 (9%,  $P_3N_3F_5CH_2^+$ ), 230 (14%,  $P_3N_3F_5^+$ ), 103 (70%, C<sub>6</sub>H<sub>5</sub>CN<sup>+</sup>), 102 (80%, C<sub>6</sub>H<sub>5</sub>C<sub>2</sub>H<sup>+</sup>), 77 (54%, C<sub>6</sub>H<sub>5</sub><sup>+</sup>).

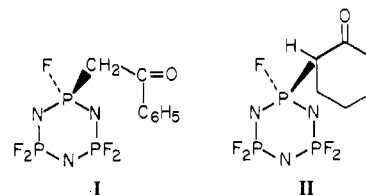
**Preparation of  $P_3N_3F_5C_6H_9O$  (II).** The same procedure was employed as the one outlined above except that cyclohexanone was used in place of acetophenone. The resulting oil was distilled at 60–70 °C and 4–5 mmHg to yield 5.2 g (33% of theory) of a water white oil. Purity, as established by VPC, was again approximately 95%. Anal. Calcd for  $P_3N_3F_5C_6H_9O$ : C, 21.95; H, 2.75; mol wt 327. Found: C, 22.00; H, 2.92; mol wt 327 (mass spectrum).

NMR:<sup>9</sup> <sup>19</sup>F  $\delta$ (PF<sub>2</sub>) 61.0 (4 F,  $J$ (PF) = 760 Hz),  $\delta$ (PFR') 59.0 (1 F,  $J$ (PF) = 765 Hz); <sup>1</sup>H  $\delta$ (CH<sub>2</sub>) 1.9 (8 H, br d),  $\delta$ (CHP) 5.5 (2 H,  $J$ (PH) = 4 Hz). IR:<sup>10</sup> 2900 (m, CH str), 2830 (w, CH str), 1680 (m, CO str), 1440 (m), 1360 (w), 1330 (w), 1270 (s, PN str), 1100 (s, PN<sup>1</sup> str), 1060 (m), 1040 (m), 1000 (m), 940 (PF asym), 840 (PF sym), 750 (PF sym), 550 (w), 500 (s), 450 (s). Mass spectra:<sup>11</sup> 327 (31%,  $P_3N_3F_5C_6H_9O^+$ ), 247 (82%,  $P_3N_3F_5OH^+$ ), 230 (20%,  $P_3N_3F_5^+$ ), 97 (9%, C<sub>6</sub>H<sub>9</sub>O<sup>+</sup>), 80 (95%, C<sub>6</sub>H<sub>8</sub><sup>+</sup>), 79 (100%, C<sub>6</sub>H<sub>7</sub><sup>+</sup>).

Both new compounds are reasonably stable under normal laboratory conditions. The expected derivatives of the ketones are formed in reactions with dinitrophenylhydrazine and butyllithium.

### Results and Discussion

The fluorine-19 NMR data indicate<sup>4</sup> the presence of the  $P_3N_3F_5$  function in both compounds I and II. The proton NMR spectra indicate substantially deshielded alkyl groups ( $\delta \sim 5.5$  ppm). The integrated areas along with the strong perturbation of the chemical shifts establish that the phosphazene moiety is attached in a position  $\alpha$  to the carbonyl function. The observation of normal ketone reactions and the ketone band in the infrared spectra reinforce this conclusion. Therefore, these molecules can be depicted as



The strong perturbation of the PCH proton chemical shifts reflects a combination of the strong electron-withdrawing effect of the  $P_3N_3F_5$  moiety<sup>12</sup> and possible anisotropic effects associated with the phosphorus atom. The difference<sup>13</sup> in  $J_{PCH}$  in the two compounds probably relates to geometric factors.

In addition to the normally expected bands from the phosphazene<sup>3</sup> and ketone functions, there are some significant perturbations in the infrared spectra of I and II. One would expect that substitution in the  $\alpha$  position of a ketone with a strong electron-withdrawing function would lead to a significant increase in the carbonyl frequency.<sup>14</sup> However, in each